

## Cyclodextrin-Triazole Derivative Functionalized on Ag–SiO<sub>2</sub> Core–Shell Nanoparticles via Click Chemistry

Gun Bae Park, Bal Sydulu Singu, Sang Eun Hong, and Kuk Ro Yoon\*

*Organic Nanomaterials Lab, Department of Chemistry, Hannam University, Daejeon 305-811, Republic of Korea. \*E-mail: kryoon@hnu.kr*

*Received May 12, 2016, Accepted July 20, 2016, Published online September 6, 2016*

Click chemistry has provided a versatile strategy for functionalization in solution chemistry under mild reaction conditions with a high degree of functional group compatibility. Initially, silver (Ag) nanoparticles were prepared by the chemical reduction method, followed by the synthesis of silver–silica (Ag–SiO<sub>2</sub>) core–shell nanoparticles by the Stöber method. The Ag–SiO<sub>2</sub> core shell nanoparticles were functionalized with the alkyne derivative. The cycloaddition reaction between the azide-functionalized cyclodextrin and the alkyne-functionalized Ag–SiO<sub>2</sub> core–shell nanoparticles was carried out via the copper-catalyzed click reaction, leading to the formation of the cyclodextrin-triazole derivative on the Ag–SiO<sub>2</sub> core–shell nanoparticles. The presence of the resulting cyclodextrin-triazole derivative on the silver–silica core–shell nanoparticles was confirmed by Fourier transform infrared spectroscopy (FT-IR), ultraviolet–visible spectroscopy (UV–vis), scanning electron microscopy (SEM), transmission electron microscopy (TEM), and thermogravimetric analysis (TGA).

**Keywords:** Silver, Silica, Core–shell nanoparticles,  $\beta$ -Cyclodextrin and triazole

### Introduction

Metal nanoparticles have attracted considerable attention both fundamentally and technologically because of their unique electronic, optical, and catalytic properties, which are not observable in their bulk counterparts. There are two reasons for this: the first is the large surface area of a nanomaterial compared to the same mass of bulk material, and the second reason is that below 50 nm the laws of physics differ from those at a larger scale.<sup>1–6</sup> The unique optical properties of metal nanoparticles arise from the collective oscillation of conduction electrons upon interaction with electromagnetic radiation, which is known as localized surface plasma resonance (LSPR).

Silver nanoparticles often show unique properties and have attracted much interest due to their large surface areas and unique physical, chemical, and biological properties, which include antibacterial activity.<sup>7,8</sup> Compared to their macroscaled counterparts, silver nanoparticles have a wide range of applications, including wound dressings, footwear, paints, cosmetics, antibacterial water filters, conductive and optical materials, catalysts, and biosensors.<sup>9,10</sup>

Silica nanoparticles have been widely used in many fields, including fillers, ceramics, colloids, polishing materials, pigments, catalysts, reinforcement materials, gene delivery, drug delivery, immunoassays, scanning probe microscopy-based imaging, and biosensing techniques. Their versatility is due to their ease of preparation by the Stöber method, which produces highly dispersed spherical silica nanoparticles,<sup>11</sup> as well as allowing the possibility of controlling the nanoparticle size, high surface area to

volume ratios, and biocompatible modified silica. The synthesis can be tailored to produce different types of inorganic nanoparticles including gold, silver, and iron oxide with a silica layer, and can be used as a direct method to obtain silica-functionalized nanoparticles. However, the hydroxyl group (–OH) on the silica surface absorbs moisture and causes agglomeration of the nanoparticles. This results in poor dispersion capacities in organic polymer matrices, limiting the applications of silica nanoparticles. The main challenge is to control particle aggregation. Fortunately, this problem can be resolved through surface modification methods utilizing polymers, surfactants, biomolecules, and functional groups. The chemical modification of the surface of silica nanoparticles with a polymer not only improves their stability but can also alter the mechanical, structural, and thermal properties of both the nanoparticle and the polymer.<sup>12–16</sup>

The goal of this study was to develop a novel and facile method to produce inexpensive silver nanoparticles surface-modified by silica with the Stöber method, yielding silver–silica (Ag–SiO<sub>2</sub>) core–shell nanoparticles and Ag–SiO<sub>2</sub> core–shell nanoparticles modified with a cyclodextrin-triazole derivative via click chemistry.

### Materials and Experimental

Silver nitrate, tetraethyl orthosilicate (TEOS), polyvinylpyrrolidone (PVP), 3-(triethoxysilyl)propyl isocyanate,  $\beta$ -cyclodextrin ( $\beta$ -CD), ethylene glycol (EG), sodium hydroxide, *p*-toluenesulfonyl chloride, sodium azide, sodium bicarbonate, copper sulfate pentahydrate, sodium

ascorbate, acetonitrile, 1,8-diaminooctane, tetrahydrofuran, propargyl alcohol, triethylamine, and trifluoromethanesulfonic anhydride were purchased from Sigma-Aldrich (Yongin, Korea). Ethanol, dichloromethane, and acetone were obtained from Samchun Pure Chemicals (Seoul, Korea). *N,N*-Dimethylformamide and ammonium hydroxide were purchased from OCI Chemicals (Seoul, Korea) and Junsei Chemicals (Chuo-ku, Tokyo), respectively. All reactions were carried out with Millipore water.

**Characterization.** Morphological analysis of the prepared materials was carried out with a field emission scanning electron microscope (FE-SEM) (Magellan 400, FEI, Oregon, USA). Transmission electron microscopy (TEM) was performed by casting sample dispersions on carbon-coated copper grids and allowing them to dry at room temperature. TEM was carried out using an FE-TEM, JEM-2100 F (HR) (JEOL Ltd, Japan). To prepare materials for Fourier transform infrared (FT-IR) analysis, they were mixed with KBr powder and compressed into pellets, with the sample powder being evenly dispersed in KBr. FT-IR spectra were recorded with an FT-IR spectrometer (model iS10, Nicolet Nexus, MN, USA). Thermogravimetric analysis (TGA) was performed on a SCINCO (TGA 1000) series thermal analyzer system at a heating rate of 10°C/min from ambient to 700°C under nitrogen atmosphere. Absorption spectra were obtained using a single-beam UV-vis spectrophotometer (Hewlett Packard 8453).

**Synthesis of Silver Nanoparticles.** Silver nanoparticles were synthesized by reducing  $\text{AgNO}_3$  with EG in the

presence of PVP (stabilization agent). In a typical synthesis, 0.75 g of PVP was dissolved in 8 mL of ethylene glycol in a two-necked, round-bottom flask at 150°C for 5 min. Silver nitrate solution (2 mL, 0.126–1.119 M in ethylene glycol) was added to the solution prepared above, and the reaction mixture was further heated at 150°C for 1 h under constant stirring. The reaction mixture was diluted with acetone and tetrahydrofuran (1:1 by volume) and centrifuged at 10 000 rpm. This centrifugation was repeated several times to remove excess EG and PVP, and the nanoparticles were finally dispersed in deionized water for storage.

**Synthesis of Ag-SiO<sub>2</sub> Core-Shell Nanoparticles.** Silver nanoparticles (8 mL, prepared as above) were placed in a 100-mL round-bottom flask and mixed with the appropriate amount of ammonia ( $\text{NH}_3$ ), ethanol, and water. The mixture was sonicated for 1 h and then a suitable amount of TEOS was added; the resulting reaction mixture was stirred for 48 h. After completion of the reaction, the mixture was centrifuged at 10 000 rpm. Centrifugation was repeated several times until the supernatant became colorless. Here it should be noted that the thickness of the SiO<sub>2</sub> shell depends on the concentration of TEOS in the reaction mixture.

**Synthesis of SiO<sub>2</sub> Nanoparticles.** Silica nanoparticles were prepared through a process based on the Stöber method: TEOS was dissolved in ethanol. Separately, ammonia water (25 wt %) and ethanol were mixed. The two solutions were combined and the resulting solution was stirred for 48 h. The particles in the solution were collected by centrifugation and dried under vacuum for 12 h.

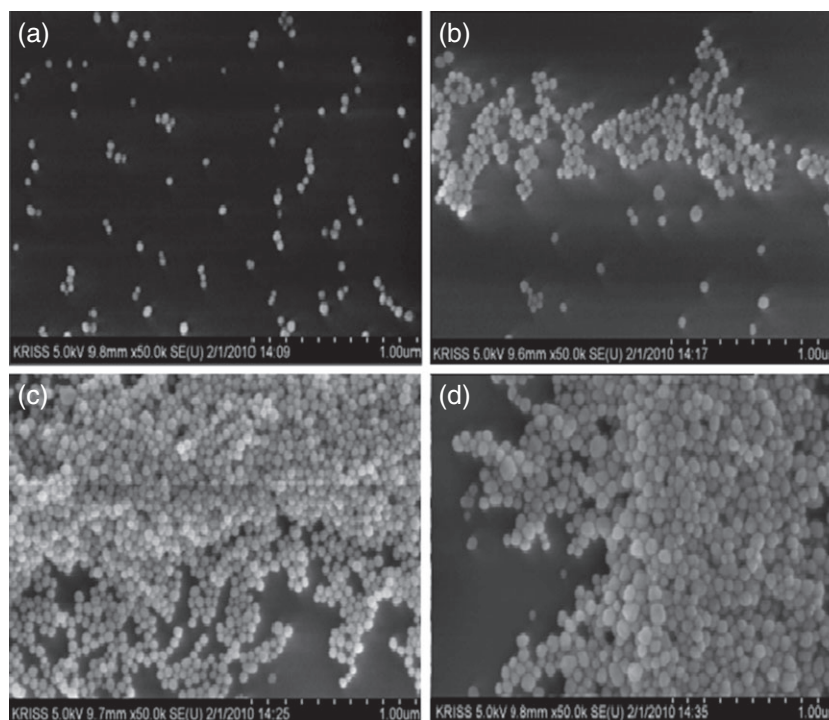


**Figure 1.** SEM images of silver nanospheres prepared at various concentrations of silver nitrate: (a) 0.126 (b) 0.253, (c) 0.503, and (d) 1.119 M.

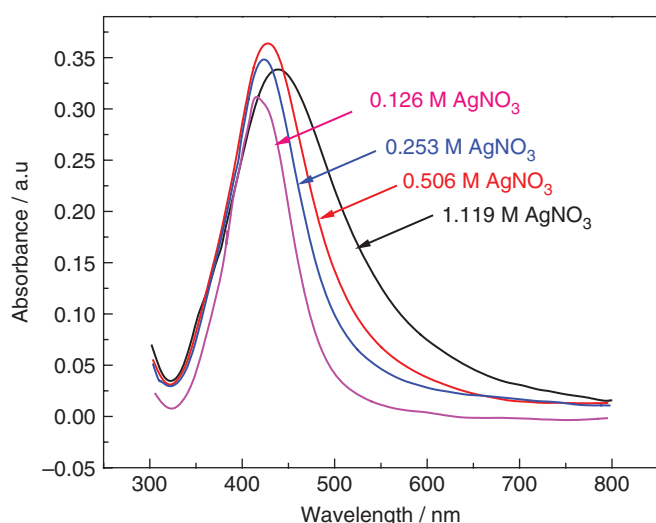


**Figure 2.** UV–vis spectra of silver nanoparticles prepared at various concentration of AgNO<sub>3</sub>.

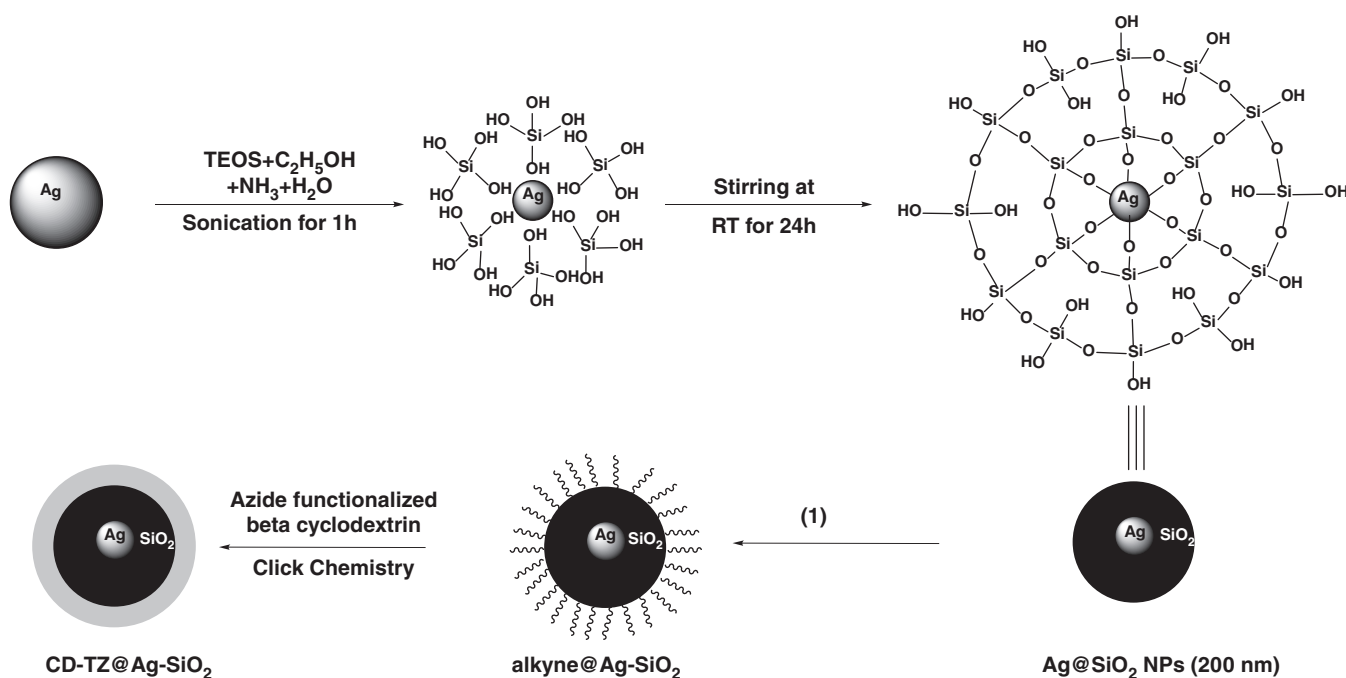
**Synthesis of Prop-2-ynyl 3-(triethoxysilyl) Propylcarbamate (1).** Propargyl alcohol (2.34 mL) and triethylamine (5.02 mL) were dissolved in 20 mL of dichloromethane (DCM) and sonicated for a few minutes, and then cooled in an ice bath for 6 h. The resulting mixture was slowly added to 3-(triethoxysilyl) propyl isocyanate (8.9 mL) in 10 mL of DCM, and then the reaction mixture was purged with nitrogen gas and stirred for 24 h. After completion, (1) was isolated as a clear, colorless, oily liquid.

**Synthesis of Alkyne-functionalized Ag–SiO<sub>2</sub> (Alkyne@Ag–SiO<sub>2</sub>) Core–Shell Nanoparticles (2).** Alkyne functionalization of Ag–SiO<sub>2</sub> core–shell nanoparticles was carried out as follows: the silver nanoparticle

dispersion solution (8 mL) was placed in a 100-mL round-bottom flask and mixed with ethanol (14 M), NH<sub>3</sub> (0.3 M), and a suitable amount of water, then sonicated for 1 h. TEOS (0.28 M) was added to the above solution and stirred for 40 min under a nitrogen atmosphere, followed by addition of 2.3 mL of prop-2-ynyl 3-(triethoxysilyl)propylcarbamate and stirring at room temperature for 36 h. After completion of the reaction, the mixture was centrifuged at 4000 rpm for 20 min, the supernatant was discarded, and (2) were washed twice with deionized water and ethanol and then dried overnight at 30°C under vacuum.

**Synthesis of Mono-6-Deoxy-6-(*p*-Tolylsulfonyl)-β-β (3).** β-CD (10.0 g, 8.81 mmol) was suspended in 80 mL of water, and NaOH (1.1 g) in 3 mL of water was added dropwise over 6 min. The suspension became homogeneous and slightly yellow before the addition was complete. *p*-Toluenesulfonyl chloride (1.68 g, 8.81 mmol) in 5 mL of acetonitrile was added dropwise over 8 min, causing the immediate formation of a white precipitate. After stirring for 2 h at 23°C, the precipitate was removed by suction filtration and the filtrate was refrigerated overnight at 4°C. The resulting white precipitate was recovered by suction filtration and dried for 12 h under vacuum, yielding the pure white solid, mono-6-deoxy-6-(*p*-tolylsulfonyl)-β-cyclodextrin (3).

**Amine-functionalized β-Cyclodextrin (Am@β-CDs) (4).** Mono (6-deoxy-6-*p*-tolylsulfonyl)-β-cyclodextrin (900 mg, 0.735 mmol) was dissolved in 1,8-diaminooctane (7.42 g, 51.45 mmol: solid at room temperature and liquid at *T* > 50°C). Some DMF was added to the above mixture until it become a uniform solution; then the reaction mixture was heated at 80°C for 12 h with constant stirring. After



**Scheme 1.** Schematic illustration of formation of β-CD-TZ@Ag–SiO<sub>2</sub>.

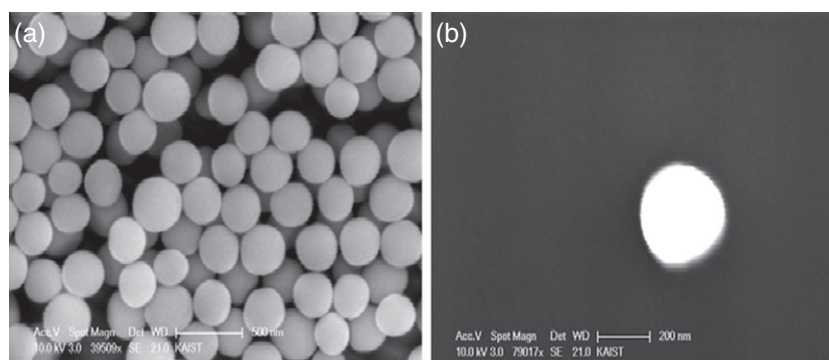


Figure 3. SEM images of SiO<sub>2</sub> nanoparticles.

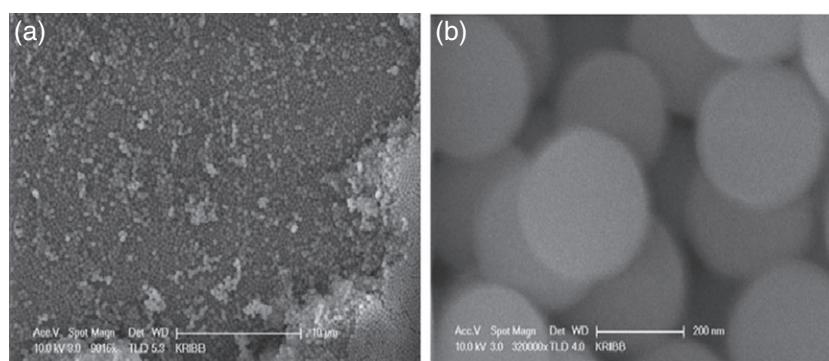


Figure 4. SEM images of  $\beta$ -CD-TZ@Ag-SiO<sub>2</sub> core-shell nanoparticles.

completion of the reaction, 10 mL of acetone was added and the precipitate was centrifuged for 10 min, after which the supernatant was discarded and the product was washed four times with acetone. Finally, the amine-functionalized  $\beta$ -cyclodextrin was dried under vacuum at 60°C (4).

**Synthesis of Azide Functionalized  $\beta$ -Cyclodextrin (Az@ $\beta$ -CDs) (5).** Am@ $\beta$ -CDs (0.4 g) were dispersed in 5.6 mL of dichloromethane and stirred for 2 h. Triflyl azide (7.0 mmol) was dissolved in 12 mL of dichloromethane and slowly injected into the Am@ $\beta$ -CDs solution. Copper sulfate (0.13 mL, 0.011 g, 0.04 mmol) solution was added to the reaction mixture, followed by stirring for 36 h at room temperature. After completion of the reaction, the product was washed with NH<sub>4</sub>OH (to remove the copper salt) followed by acetone to obtain the Az@ $\beta$ -CDs (5).

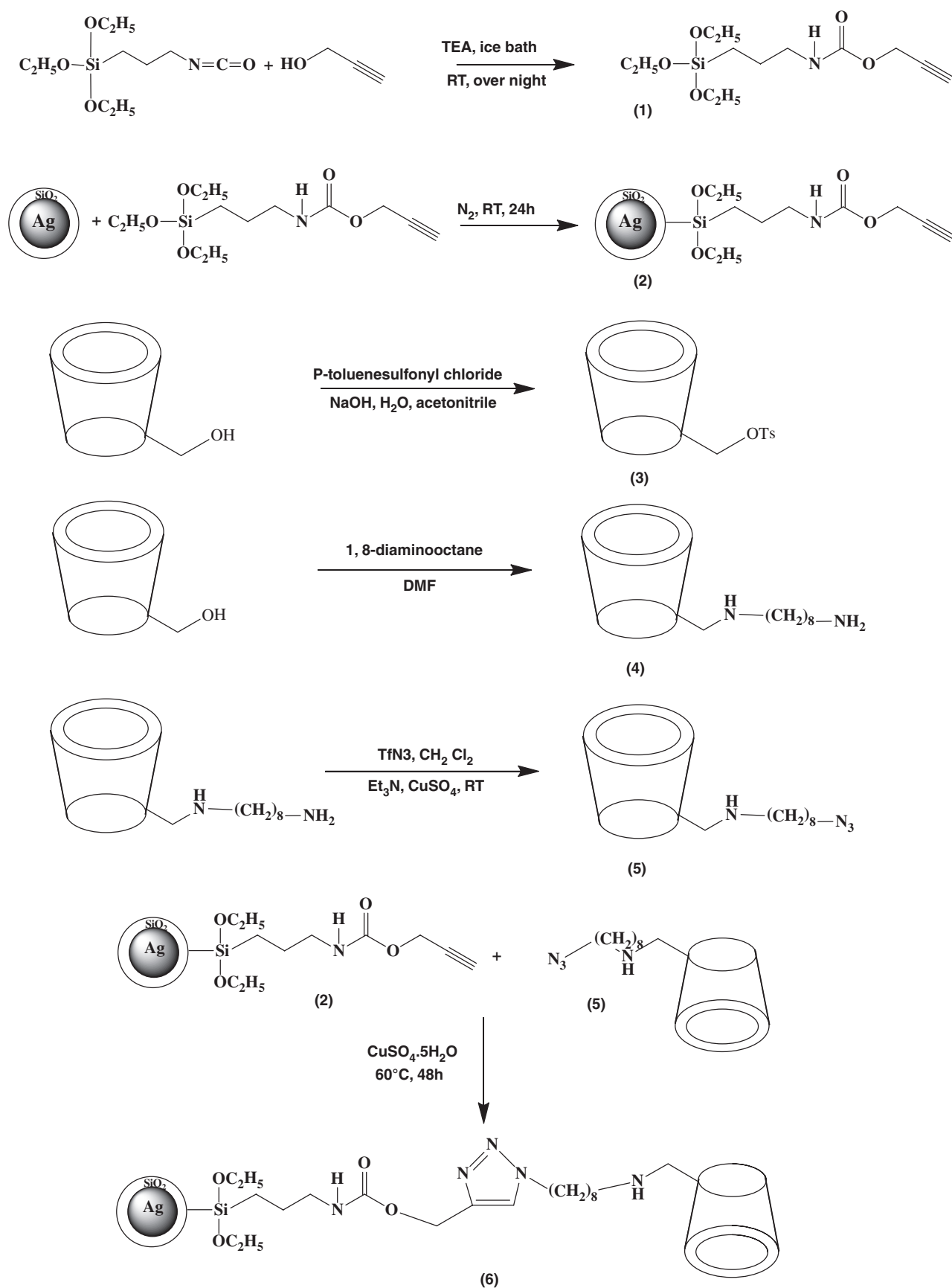
**Synthesis of  $\beta$ -Cyclodextrin-Triazole Derivative Functionalized Ag-SiO<sub>2</sub> ( $\beta$ -CD-TZ@Ag-SiO<sub>2</sub>) Core-Shell Nanoparticles Via Click Chemistry (6).** The click reaction was carried out between the alkyne@Ag-SiO<sub>2</sub> core-shell nanoparticles and Az@ $\beta$ -CDs as follows: the dried alkyne@Ag-SiO<sub>2</sub> core-shell nanoparticles were dispersed in 30 mL of methanol and sonicated for 10 min. Solutions of Az@ $\beta$ -CDs (0.87 g, 0.75 mmol, excess) in 28 mL deionized water, sodium ascorbate (0.03 g, 0.15 mmol, dissolved in 1 mL water), and CuSO<sub>4</sub>·5H<sub>2</sub>O (0.019 g, 0.075 mmol, dissolved in 1 mL water) were added. The reaction mixture was stirred for 48 h at room temperature, after which the product was recovered by vacuum filtration,

washed with NH<sub>4</sub>OH to remove the copper sulfate salt, and further washed several times with deionized water. Finally, the  $\beta$ -CD-TZ@Ag-SiO<sub>2</sub> core-shell nanoparticles were recrystallized from acetone.

## Results and Discussions

Silver nanoparticles were synthesized by the reduction of silver nitrate using ethylene glycol in the presence of PVP. The microstructure of the silver nanoparticles was analyzed by SEM (Figure 1), which confirmed the formation of uniform nanospheres. When the concentration of silver nitrate was increased from 0.126 to 1.119 M, the silver nanosphere size increased from 20 to 64 nm.

The changes in the optical properties of the PVP-capped silver colloid solutions were recorded using a UV-visible spectrophotometer (Figure 2). The UV-vis spectra show single, broad, well-defined, asymmetric peaks with maximum absorbances at 420, 423, 428, and 440 nm, which are due to the surface plasmon absorption of the colloidal silver nanoparticles. The positions of the surface plasmon absorption peaks of spherical silver nanoparticles depend on the refractive index of the medium, the particle size, and the capping groups on their surfaces. The UV-vis spectra presented in Figure 2 clearly show a red shift as the concentration of silver nitrate was increased from 0.126 to 1.119 M, which is due to the increased size of the nanoparticles, in agreement with the SEM morphology results shown in Figure 1.



**Scheme 2.** Synthesis of prop-2-ynyl 3-(triethoxysilyl) propylcarbamate (1), alkyne@Ag-SiO<sub>2</sub> (2), mono-6-deoxy-6-(*p*-tolylsulfonyl)- $\beta$ -cyclodextrin (3), Am@ $\beta$ -CDs (4), Az@ $\beta$ -CDs (5), and  $\beta$ -CD-TZ@Ag-SiO<sub>2</sub> (6).

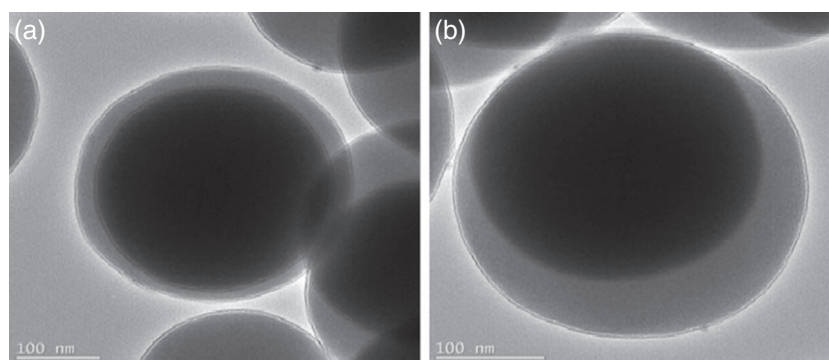


Figure 5. TEM images of  $\beta$ -CD-TZ@Ag-SiO<sub>2</sub> core-shell nanoparticles.

Ag-SiO<sub>2</sub> core-shell nanoparticles were synthesized by the Stöber method using Ag nanoparticles as the core (60 nm), as shown in Scheme 1. The morphology of the pure SiO<sub>2</sub> nanoparticles is shown in Figure 3 (prepared without the Ag nanoparticles). From the SEM analysis, the average size of the SiO<sub>2</sub> nanoparticles was found to be ~210 nm.

Figure 4 shows the SEM images of  $\beta$ -CD-TZ@Ag-SiO<sub>2</sub> core-shell nanoparticles, the synthesis of which is illustrated in Scheme 2. The  $\beta$ -CD-TZ@Ag-SiO<sub>2</sub> core-shell nanoparticles were found to be 210 nm in size, whereas the average size of the Ag-SiO<sub>2</sub> core-shell nanoparticles was found to be 190 nm.

TEM images of the  $\beta$ -cyclodextrin-azide derivative-functionalized Ag-SiO<sub>2</sub> core-shell nanoparticles are shown in Figure 5. This confirms that the shell was formed on addition of the  $\beta$ -cyclodextrin-azide derivative to Ag-SiO<sub>2</sub> core-shell nanoparticles, and the thickness of the  $\beta$ -cyclodextrin-azide derivative layer was 10–20 nm.

UV-vis absorption spectra of silver, SiO<sub>2</sub>, and  $\beta$ -CD-TZ@Ag-SiO<sub>2</sub> core-shell nanoparticles are shown in Figure 6. The UV-vis spectra of silver and SiO<sub>2</sub> nanoparticles show peaks at 438 and 254 nm (Figure 7). The UV-vis spectra of Ag nanoparticles and  $\beta$ -CD-TZ@Ag-SiO<sub>2</sub> core-shell nanoparticles exhibit peaks at 438 and 290 nm, the blue shift possibly being due to the addition of the functionalized  $\beta$ -cyclodextrin-azide derivative to the surface of the nanoparticles, as confirmed by TEM analysis (Figure 5). A similar blue shift was reported by Herrera *et al.* when silver nanoparticles were modified with  $\alpha$ -cyclodextrin.<sup>17</sup>

Figure 8 shows the thermograms of Ag-SiO<sub>2</sub> and alkyne@Ag-SiO<sub>2</sub> core-shell nanoparticles. After completion of the pyrolysis at 700°C, there was a 2 wt % loss difference between the Ag-SiO<sub>2</sub> and alkyne@Ag-SiO<sub>2</sub> core-shell nanoparticles. The larger weight loss in case of the alkyne@Ag-SiO<sub>2</sub> was due to the presence of the alkyne derivative on the Ag-SiO<sub>2</sub> core-shell nanoparticles, as was previously confirmed by SEM analysis.

Figure 9 shows the thermograms of the alkyne@Ag-SiO<sub>2</sub> and  $\beta$ -CD-TZ@Ag-SiO<sub>2</sub> core-shell nanoparticles. After completion of pyrolysis (700°C),  $\beta$ -CD-TZ@Ag-SiO<sub>2</sub> showed an 18 wt % increase in weight loss compared to the alkyne@Ag-SiO<sub>2</sub> core-shell nanoparticles, which is due to

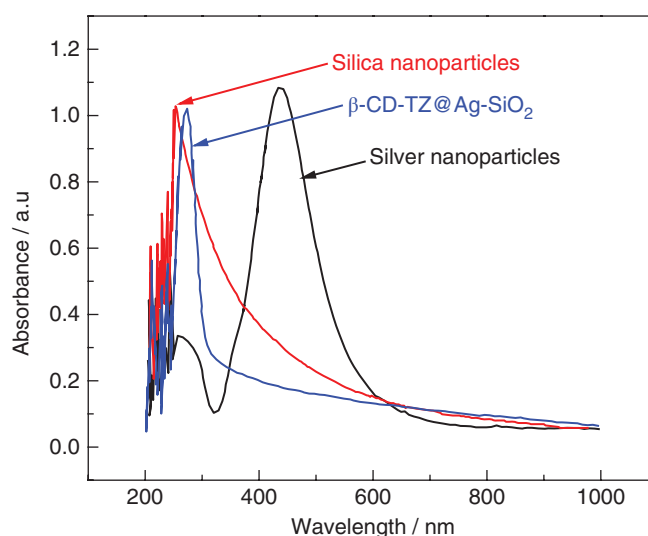


Figure 6. UV-vis spectra of silver, SiO<sub>2</sub>, and  $\beta$ -CD-TZ@Ag-SiO<sub>2</sub> core-shell nanoparticles.

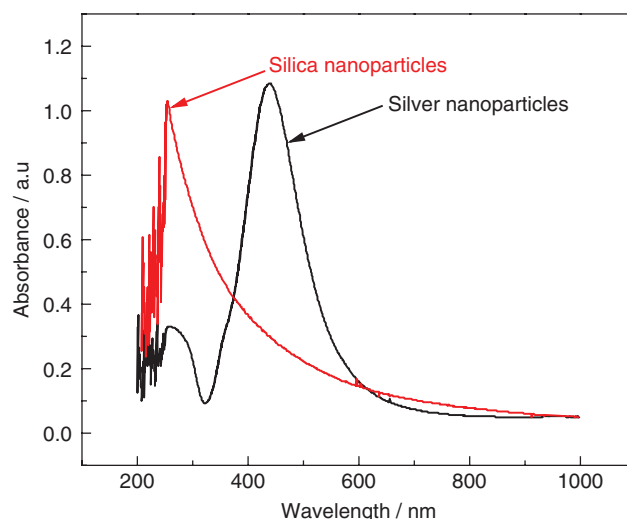
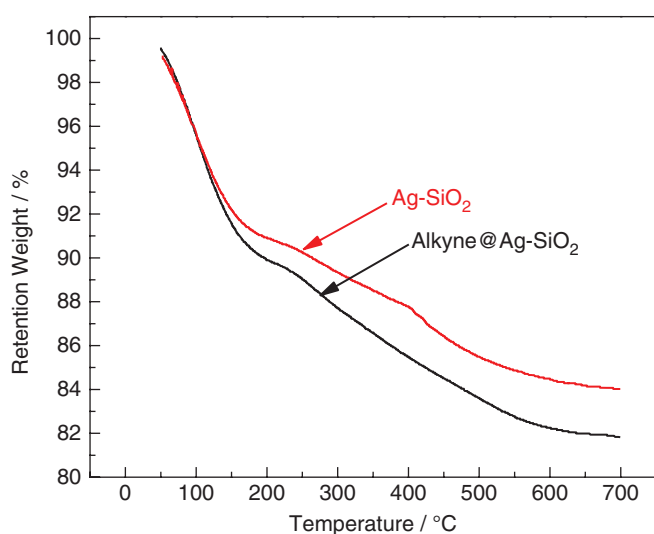
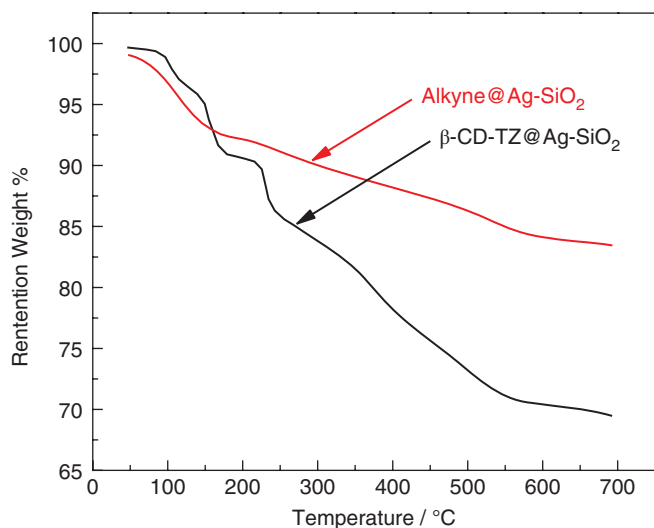


Figure 7. UV-vis spectra of silver and SiO<sub>2</sub> nanoparticles.

the higher molecular weight of the functionalized  $\beta$ -cyclodextrin-triazole derivative on the Ag-SiO<sub>2</sub> core-shell nanoparticles. The thermal analysis confirmed that the surface of



**Figure 8.** Thermograms of (i) Ag-SiO<sub>2</sub> and (ii) alkyne@Ag-SiO<sub>2</sub> core-shell nanoparticles.



**Figure 9.** Thermograms of (i) alkyne@Ag-SiO<sub>2</sub> and (ii)  $\beta$ -CD-TZ@Ag-SiO<sub>2</sub> core-shell nanoparticles.

the Ag-SiO<sub>2</sub> core-shell nanoparticles was functionalized with the alkyne and  $\beta$ -cyclodextrin-triazole derivatives.

Figure 10(a) shows the FT-IR spectra of the Az@ $\beta$ -CDs, which show peaks at 3440 and 2924 cm<sup>-1</sup> corresponding to N-H and C-H stretching bands, respectively. The peak at 2120 cm<sup>-1</sup> is due to the stretching band of the azide functional group, while the peak at 1152 cm<sup>-1</sup> relates to the stretching band of the C-N bond. The FT-IR spectrum of the  $\beta$ -CD-TZ@Ag-SiO<sub>2</sub> core-shell nanoparticles is shown in Figure 10(b). The spectrum shows peaks at 3462 cm<sup>-1</sup> (N-H stretching), 2930 cm<sup>-1</sup> (Ar-CH stretching), 1694 cm<sup>-1</sup> (C=O stretching), 1633 cm<sup>-1</sup> (C=C stretching), 1583 cm<sup>-1</sup> (C-N stretching), 1433 cm<sup>-1</sup> (N=N stretching), 1071 cm<sup>-1</sup> (Si-O-Si stretching), 880 cm<sup>-1</sup> (CH<sub>2</sub>-R<sub>2</sub>C stretching), and 831 cm<sup>-1</sup> (C-N stretching). These values are in accordance with those reported in the literature.<sup>18</sup>

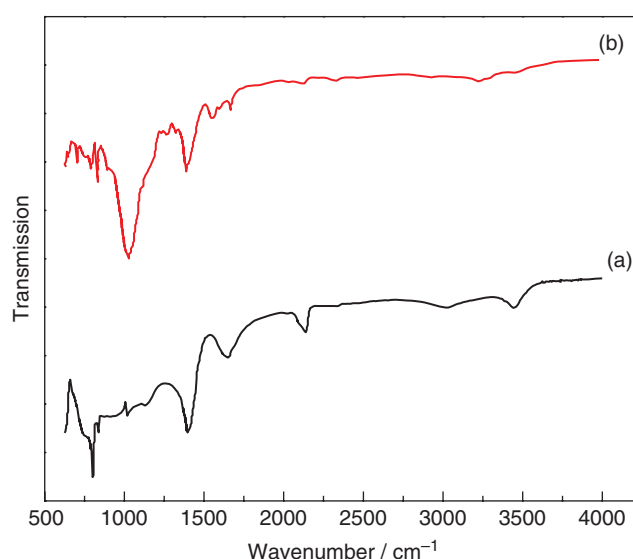


**Figure 10.** FT-IR spectra of (a) Az@ $\beta$ -CDs and (b)  $\beta$ -CD-TZ@Ag-SiO<sub>2</sub> core-shell nanoparticles.

Comparing the FT-IR spectra of Az@ $\beta$ -CDs and  $\beta$ -CD-TZ@Ag-SiO<sub>2</sub>, it can be seen that in Az@ $\beta$ -CDs the band at 2120 cm<sup>-1</sup> (stretching of the azide) has disappeared on conversion to  $\beta$ -CD-TZ@Ag-SiO<sub>2</sub> via the click reaction of Az@ $\beta$ -CDs and alkyne@Ag-SiO<sub>2</sub>, which also caused the formation of new bands at 1633, 1583, and 1433 cm<sup>-1</sup> related to the newly formed triazole C=C, C-N, and N=N bonds, respectively.<sup>19,20</sup>

## Conclusions

Silver nanoparticles were successfully prepared using a chemical reduction method in the presence of PVP dispersant. The average size of the silver nanoparticles ranged from 20 to 64 nm, with corresponding UV-vis absorption maxima at 415–430 nm.

The Ag-SiO<sub>2</sub> core-shell nanoparticles were prepared by the Stöber method using TEOS. Well-defined  $\beta$ -CD-TZ@Ag-SiO<sub>2</sub> core-shell nanoparticles were prepared from Az@ $\beta$ -CDs and alkyne@Ag-SiO<sub>2</sub> via the click reaction.

**Acknowledgment.** Publication cost of this article was supported by the Korean Chemical Society.

## References

1. A. Dowling, Report by The Royal Society and The Royal Academy of Engineering, London, July, **2004**.
2. S. D. Bhagat, Y. H. Kim, K. H. Suh, Y. S. Ahn, J. G. Yeo, J. H. Han, *Micropor. Mesopor. Mater.* **2008**, *112*, 504.
3. Y. L. Lee, Z. C. Du, W. X. Lin, Y. M. Yang, *J. Colloid Interface Sci.* **2006**, *296*, 233.
4. Y. Ouabbas, A. Chamayou, L. Galet, M. Baron, G. Thomas, P. Grosseau, B. Guilhot, *Powder Technol.* **2009**, *190*, 200.
5. C. Oh, Y. G. Lee, C. U. Jon, S. G. Oh, *Colloids Surf. A* **2009**, *337*, 208.

6. M. Castellano, L. Conzatti, G. Costa, L. Falqui, A. Turturro, B. Valenti, F. Negroni, *Polymer* **2005**, *46*, 695.
7. C. Noguez, *J. Phys. Chem. C* **2007**, *111*, 3806.
8. N. M. Bahadur, T. Furusawa, M. Sato, F. Kurayama, I. A. Siddiquey, N. Suzuki, *J. Colloid Interface Sci.* **2011**, *355*, 312.
9. D. V. Quang, P. B. Sarawade, A. Hilonga, J. K. Kim, Y. G. Chai, S. H. Kim, J. Y. Ryu, H. T. Kim, *Appl. Surf. Sci.* **2011**, *257*, 6963.
10. A. A. Okeil, A. Amr, F. A. A. Mohdy, *Carbohydr. Polym.* **2012**, *89*, 1.
11. S. Fazzini, M. C. Cassani, B. Ballarin, E. Boanini, J. S. Girardon, A. S. Mamede, A. Mignani, D. Nanni, *J. Phys. Chem. C* **2014**, *118*(42), 24538.
12. H. Zou, S. Wu, J. Shen, *Chem. Rev.* **2008**, *108*(9), 3893.
13. B. Radhakrishnan, R. Ranjan, W. J. Brittain, *Soft Matter* **2006**, *2*(5), 386.
14. X. Chen, Y. F. Huang, W. Tan, *J. Biomed. Nanotechnol.* **2008**, *4*(4), 400.
15. P. Tallury, K. Payton, S. Santra, *Nanomedicine* **2008**, *3*(4), 579.
16. G. Kickelbick, *Prog. Polym. Sci.* **2002**, *28*(1), 83.
17. B. Herrera, T. Bruna, D. Guerra, N. Yutronic, M. J. Kogan, P. Jara, *Adv. Nanopart.* **2013**, *2*, 112.
18. K. A. Perrinea, V. T. Andrew, *Chem. Soc. Rev.* **2010**, *39*, 3256.
19. H. Li, Q. Zheng, C. Han, *Analyst (Cambridge, U. K.)* **2010**, *135*, 1360.
20. S. Zhai, Y. Ma, Y. Chen, D. Li, J. Cao, Y. Liu, M. Cai, X. Xie, Y. Chen, X. Luo, *Polym. Chem.* **2014**, *5*, 1285.